Amorphous silica and the intergranular structure of nanocrystalline silica

Edgar R. van Hoek & Rudolf Winter

Department of Physics, University of Wales Aberystwyth, Penglais, Aberystwyth, SY23 3BZ, Wales, UK

Abstract

In the present study, the local structure of nanocrystalline SiO_2 with varying particle size, obtained by high-energy ball-milling, is compared with coarse-grained quartz and commercial amorphous fused-silica nano-particles. The average grain size of the nanocrystalline samples is determined by x-ray diffraction, and decreases with milling time down to about 5 nm.

Both x-ray diffraction (XRD) and ^{29}Si magic-angle spinning (MAS) nuclear magnetic resonance (NMR) signals split into narrow and broad components after several hours of ball milling. On the basis of line shape analysis of diffractograms and spectra, the progressive effect of ball milling on the structure is described in terms of a two-stage process involving the formation of wide-angle grain boundaries and subsequent pressure-amorphisation.

An in-situ annealing experiment tracked by XRD reveals that the effect of the first stage is reversible at moderate temperature, while the second stage, which transforms the powder into a nanocrystalline material with grain and intergranular components, is not reversible at temperatures up to $1\,025°C$.

Introduction

The structure of the grain-matrix interface in a glass-forming mixture determines both the growth of precipitates in the glass body and the dissolution rate of raw material particles in the melt[1]. Due to their small size, nanocrystals have a large surface-to-volume ratio; they are therefore regarded as a good model system if the interface structure is to be studied with bulk techniques. The intergranular structure in a nanocrystalline compound can, however, itself be disordered, and the question arises whether the intergranular material is related to conventional glassy forms of the same composition.

Nanocrystalline materials consist of highly-ordered crystalline grains in a disordered matrix. Many properties specific to this material class are due to the reduced particle size and the heterogeneously disordered structure. Several model assumptions for the type of disorder present in the grain boundaries have been suggested[2, 3], including a glass-like amorphous structure, a gradient structure, and the mere presence of wide-angle boundaries between adjacent grains. The interface fraction, *i.e.* the amount of material located in grain boundaries, is a function of both particle size and shape. It is possible to derive morphological models of the intergranular structure if independent measurements of the particle size and the interface fraction are available[4]. In the present work, the former is achieved by analysing x-ray diffraction line broadening, while the latter is obtained by NMR line shape analysis.

The presence of particles in silicate glasses (due to phase separation, as a consequence of incomplete melting of raw products, or deliberately dispersed to form glass ceramics) and their stability in the glassy matrix are an issue in both materials science and industrial glass production. Since dissolution and growth are interface-dominated processes, reliable models of the grain-matrix interface are crucial if inhomogeneities are to be avoided or controlled. In the present study, the structure of the intergranular material in nanocrystalline silica is compared to that of bulk amorphous silica.

Early reports on the amorphisation of ground quartz found by differential thermal analysis have been contradicted by x-ray diffraction almost 30 years ago[5]. It seems, however, that the grinding conditions used at the time were much less severe than those available now, and mechanical amorphisation is achievable if the energy per impact is maximised. The fact that phase transitions in nanocrystalline silica

2

are not necessarily the same as in coarse-grained variants, especially if surface stress relaxation plays a role, has recently been shown by a study on a nanocrystalline mineral form of quartz, agate[6].

Experimental

Nanocrystalline silica was prepared from polycrystalline powder (Aldrich) by ball milling using a double Spex 8000 high-energy mill with corundum vials and one 8 mm corundum ball. Milling times range from 10 minutes to 128 hours. The vials and balls were dried in an oven at 120°C for at least 30 min. Each ball-milling run produced about 2x2 g nanocrystalline silica. The weight of the sample and the ball were recorded before and after each run. There is no indication that noticeable amounts of container or ball material is abraded and mixed into the samples; no alumina reflections are found in diffractograms either.

X-ray diffractograms were recorded on a diffractometer equipped with an Enraf Nonius Cu rotating anode at the Materials Science Laboratory (MSL) at Daresbury. This diffractometer operates in transmission geometry and records a scattering angular range from $\approx 5°(2\theta)$ to $\approx 80°(2\theta)$ simultaneously using a linear detector array. Data were accumulated for 15 min. MSL software was used to unsmear the readings from the individual detector channels. XRD samples on the rotating anodes were free-standing pellets of 13 mm diameter and approximately 250μm thickness. These were produced in a uniaxial die press at a load of 3 metric tons. For some of the samples prepared with short milling times, a Siemens Kristalloflex Cu sealed-tube diffractometer in conventional θ–2θ setup was used because of its higher angular resolution. In this case, uncompacted powder was poured into a mould in an aluminium sample holder. All diffractograms were angle-calibrated with Si as external standard. Angle-dependent background was subtracted prior to analysis of the data. In addition, in-situ annealing experiments were carried out on the rotating-anode diffractometer with heating rates ranging from 2 K/min to 15 K/min and up to a maximum temperature of 1025°C. Here, data were accumulated for 1 min to 6 min per scan dependent on the heating rate.

^{29}Si magic-angle spinning NMR spectra were obtained on a Bruker Avance DSX 400 spectrometer and a Bruker 9.4 T cryomagnet. The sample powder was placed inside standard 4 mm ZrO_2 MAS rotors, which were spun at a rate of 5 kHz in a standard Bruker MAS probe. While the $\pi/2$ pulse length is 1.4 μs, a pulse

angle of approximately 30° was typically used, with a spectral width of about 780 kHz, while 4 096 data points were recorded per free induction decay. The recycling delay was 400 s since the absence of paramagnetic centres accounts for an unusually long relaxation time. 140 scans were needed to achieve a signal-to-noise ratio sufficient for the analysis undertaken in this study.

Results

X-ray diffractograms of uncrushed ("raw") quartz and ball-milled product after 16 and 32 hours are shown in the upper section of Fig. 1. After 16 hours, all quartz lines are still clearly visible, although they are broadened. In addition, a broad background underneath the peaks remains in the diffractograms of the crushed samples after subtraction of the angle-dependent background due to the scattering geometry. The 32-hour diffractogram shows a considerably smaller peak intensity and a larger background. While it cannot be expected that the total (integrated) intensities of all diffractograms are identical since the sample thickness and the powder density are not known exactly, the decrease in peak height still indicates both the broadening of the peaks and the increase of the broad background.

The average particle size was determined from the diffractograms by applying the Scherrer formula[7],

$$d = k\lambda \ / \ (\sqrt{B_n^2 - B_p^2}\cos\theta) \qquad , \qquad (1)$$

with λ the wavelength, B_n and B_p the diffraction line width of the $n$ano-and the $p$olycrystalline material, θ the Bragg angle, and the particle shape factor $k \approx 0.9$, which is a likely value for compact particles with a shape distribution[7]. X-ray diffraction line broadening reveals the size of crystalline domains. These domains can form agglomerates of considerably larger size as can be shown by small-angle scattering [8]. Ball milling breaks crystals up into smaller crystallites by formation of wide-angle grain boundaries. This mechanism leads to the formation of agglomerate particles with a crystallite substructure with disordered wide-angle grain boundary material at the interface between crystallites. A first effect on the particle size of the grinding process can be measured after 2 hours milling time. Based on the strongest peak, the (101) reflection, the particle size decreases down to about 5 nm after 16 hours milling. Further milling hardly increases the broadening effect on this line, but causes the intensity of the line to drop in favour

4

of the background. A magnification of the area around the strongest lines is shown in the bottom part of Fig. 1. It becomes clear that almost all scattered intensity is in the broad background signal after 128 hours of grinding.

A similar trend is observed in ^{29}Si NMR spectra (Fig. 2). The narrow line originating from silicon nuclei in a crystalline environment is progressively superposed by a broad component. This is already apparent after short milling times, but the superposition nature rather than a simple peak broadening, *i.e.* the non-Gaussian line shape, becomes obvious after 8 hours for the first time. After 16 hours, the chemical shifts of the two components can be distinguished, the broad component being centred at less negative values. After 64 hours, the narrow line is finally indistinguishable, and only the broad one remains.

The drastic impact ball milling has on the NMR line shape is traced in Fig. 3. A spectrum obtained at the intermediate stage, *i.e.* with both components present, is compared to the spectra of coarse-grained quartz and amorphous fused-silica nanoparticles (the latter spectrum being similar if not identical to that of bulk silica glass). The shifts of the coarse-grained material, the amorphous reference, and the narrow component in the nanocrystalline sample are very similar, while the broad component is shifted to less negative shift values. If approximated with Gaussian lines, even the narrow component is considerably broader than the coarse-grained reference line. The full width at half magnitude of the broad line of the ground sample is significantly larger than that of the amorphous sample.

The results of a rapid (15 K/min) in-situ annealing experiment monitored by diffraction is shown in Fig. 4. The diffractogram does not change dramatically below 240°C. In the temperature range from 240°C to 480°C, a shoulder near the quartz (101) scattering angle emerges and evolves into a small but distinctive peak on top of the broad signal of the ball-milled material. The broad line itself narrows in the same temperature range, and its centre moves to the position of the quartz (100) line. Above 480°C, the line shape does not change any more, and even prolonged heating at 1025°C does not have any further effect. The phase transition from alpha-quartz to beta-quartz at 573°C is not picked up since the two strongest lines do not move at the transition within the accuracy in this rather coarse in-situ experiment.

Discussion

In both XRD and NMR, disordered environments can be distinguished from ordered settings since they exhibit broadened line shapes. In diffraction, this is due to a less well-defined Bragg condition, *i.e.* a reduction in the number of lattice planes interfering positively. In NMR, the line broadening simply reflects the distribution of environments with different electron density and hence chemical shift. If a nanocrystalline material is modelled as an ensemble of small crystalline grains in an amorphous matrix, then a narrow NMR line on top of a broad one is expected as well as the simultaneous occurrence of a somewhat broadened crystalline reflection and a very broad amorphous background in the diffractogram.

At first sight, all these expectations are indeed confirmed in this study, as Figs. 1 and 2 show. Beyond this, it is possible to draw some conclusions on the nature of the disordered interface structure if the data are analysed in detail. The effect of ball milling seems to occur in two stages: A continuous diffraction line broadening is observed until after 16 hours a Scherrer estimate of about 5 nm is reached. After that, only the most prominent diffraction lines remain visible while their line width does no longer change very much. Simultaneously, a broad background arises which may be considered as the hallmark of a glass-like First Sharp Diffraction Peak ("sharp" compared to reflections from an amorphous structure, but broad compared to crystalline lines). Hence the first stage splits crystalline grains up into smaller units, thereby reducing the size of regions capable of constituting a Bragg condition, while in the second stage, the crystalline order collapses altogether. The few remaining crystallites give rise to the two sharp reflections in the 32-hour diffractogram, while the intensity of the weaker lines is no longer sufficient to rise above the noise. After 128 hours, the sample seems to be completely amorphised. This two-stage process can also be deduced from the NMR spectra (Fig. 2), where initially only a slight broadening near the base of the spectral line is observed. If, as a consequence of the mechanical impact, wide-angle grain boundaries are initially formed inside the grains, then the local site symmetry is not changed very much, but the long-range translational symmetry relevant to diffraction is broken already. Consequently, the shape of the entire diffraction line is affected, while only the base of the NMR line reflects the structural change. After 8 hours of ball milling, the NMR line is still symmetric. Between 8 and 16 hours of milling, the transition from stage 1 to stage 2 takes place. As a consequence, another very broad

6

line appears in the NMR spectrum, at less negative shift values. This line cannot be explained in terms of added grain boundaries, but a second -amorphous- phase has to be assumed. This marks the transition from a powder to a nanocrystalline material comprising both a grain component and an intergranular component.

A more detailed study of the NMR line shapes (cf. Fig. 3) clearly shows that the two components of the nanocrystalline silica spectrum (after 32 hours milling) are shifted with respect to each other. Comparing the chemical shifts of amorphous silica (top, -114.5 ppm), the grain material in the nanocrystalline sample (centre, -113.6 ppm), and coarse-grained crystalline silica (bottom, -112.7) reveals that all shifts are similar. The chemical shift of the grain-boundary component of the nanocrystalline material, however, is considerably smaller (-109.4 ppm). A compilation[9] of chemical shift values of various pressure-amorphised silica variants is reprinted in Table 1. It appears that the move of the intergranular line to less negative shift values is due to some form of mild compression as a consequence of the mechanical impact. Since the Si-O bond length is generally constant and Si is not normally found in non-tetrahedral environments in amorphous silicates, the change in position is most likely due to an increased bond-angle disorder[10], which is indeed reflected by the width of the line. The line width of the intergranular peak (20 ppm) is even larger than line widths of fully interconnected SiO_4 tetrahedra ("Q^4 species") usually found in silicate glasses[1, 11, 12] and also here in the amorphous sample (13 ppm). The bond-angle distribution in the intergranular material is therefore much wider than that in glass prepared through the melt, and even wider than in most pressure-amorphised forms[9]. It must be noted, however, that this distribution is the average over a macroscopic sample, and it cannot be taken for granted that all parts of the sample have been subject to the same total impact since part of the sample tends to stick to the walls of the vials.

The narrow component of the nanocrystalline spectrum is also wider than the polycrystalline line, indicating that even the bulk material shows some degree of disorder. In accordance with the two-stage model, this is due to the increased fraction of Si atoms in the vicinity of the surface of the crystalline grains, *i.e.* those atoms whose environment changes when wide-angle grain boundaries are formed without destroying the local crystal-like arrangement of atoms. The narrow spectral component does not fit the crystalline peak in Fig. 3 perfectly. On top of the line, there is an additional spike which has the same position and width

as the coarse-grained reference. On the basis of the two-stage model, the spins contributing to this unbroadened line can be attributed to those sites which are located in the undisturbed cores of grains. Unfortunately, the signal-to-noise ratio does not allow to quantify this interpretation at present.

The annealing experiment on a sample whose diffractograms and spectra suggest that it is virtually completely amorphised (Fig. 4) reveals that a limited amount of crystalline order can be restored. The strong (101) reflection re-appears at moderate temperature. However, only a small fraction of the total scattered intensity is found in this crystalline line. Most atoms remain in an amorphous environment even after extended treatment at $1\,025°C$. The amorphous background decreases in width, indicating that the bond-angle disorder is relaxed with annealing. Hence it appears that the first stage (formation of wide-angle grain boundaries) is reversible while the second stage (amorphisation) is not.

It has been suggested that water is accumulated by adsorption in fine-grained quartz[5]. This cannot be ruled out in this case. There is, however, no indication of water being chemically incorporated in the structure in significant amounts since this would require that non-bridging oxygens (NBO's) are formed. Tetrahedrally coordinated Si with one NBO (a "Q^3 species") generally appears at around -90 ppm in the NMR spectrum. This is at the fringe of the broad line attributed to the nanocrystalline intergranular component, and therefore water cannot account for much of the line.

Conclusion

The ball-milling process has a two-stage impact on the structure of ground silica. First, wide-angle grain boundaries are introduced by mechanical attrition, leading to a broadening of the x-ray reflections and the formation of a slightly broadened component near the base of the NMR line due to Si atoms in distorted near-surface sites. This process is reversible if the samples are annealed at moderate temperature. In the second stage, the powder is transformed into a nanocrystalline material with grains embedded in an amorphous matrix. The structure of the amorphous matrix is more disordered (in terms of a bond-angle distribution) than fused silica; it rather resembles silica pressure-amorphised under moderate conditions. The second stage of the mechanical effect of ball milling is not reversible at temperatures up to $1\,025°C$, although a structural relaxation of the bond-angle disorder of the

intergranular material is observed.

References

[1] AR Jones, R Winter, GN Greaves, C Targett-Adams, IH Smith, *Glass Technology* (accepted) ,

[2] H Gleiter, *Phys Stat Solidi* (1992) **B172**, 41

[3] RW Siegel, *Encycl Appl Phys* (1994) **11**, 173

[4] R Winter, P Heitjans, *J Non-Cryst Solids* (2001) **293**, 19

[5] GSM Moore, HE Rose, *Nature* (1973) **242**, 187

[6] S Rios, EKH Salje, SAT Redfern, *Eur Phys J* (2001) **B20**, 75

[7] HP Klug, LP Alexander, *X-ray Diffraction Procedures*, Wiley, New York, 1974

[8] R Winter, M Quinten, A Dierstein, R Hempelmann, A Altherr, M Veith, *J Appl Cryst* (2000) **33**, 507

[9] PS Fiske, WJ Nellis, Z Xu, JF Stebbins, *Am Mineral* (1998) **83**, 1285

[10] H Maekawa, P Florian, D Massiot, H Kiyono, M Nakamura, *J Phys Chem* (1996) **100**, 5525

[11] F Meneau, R Winter, GN Greaves, Y Vaills, *J Non-Cryst Solids* (2001) **293**, 693

[12] CI Merzbacher, BL Sherriff, JS Hartmann, WB White, *J Non-Cryst Solids* (1990) **124**, 194

Table 1: Chemical shifts in various forms of pressure-amorphised SiO_2 (quoted from[9]), and the various shifts found in this study.

fused at room pressure	-111.5 ppm
quenched, 6 GPa	-108.5 ppm
cold compressed, 18 GPa	-105.6 ppm
hot compressed, 5 GPa	-108.5 ppm
diaplectic (shocked)	-107.8 ppm
amorphous nanoparticles	-114.5 ppm
nanocrystalline grain component	-113.6 ppm
coarse-grained quartz	-112.7 ppm
nanocrystalline intergranular component	-109.4 ppm

Figure captions:

Fig. 1: X-ray diffractograms of silica particles. Top: Raw material, ball-milled material after 16 and 32 hours. Bottom: Evolution of the two strongest lines and collapse of the structure after 128 hours of grinding. (In both plots, the angle scale corresponds to the bottom diffractogram only; all other diffractograms are progressively shifted by 2 deg each as indicated by the broken lines).
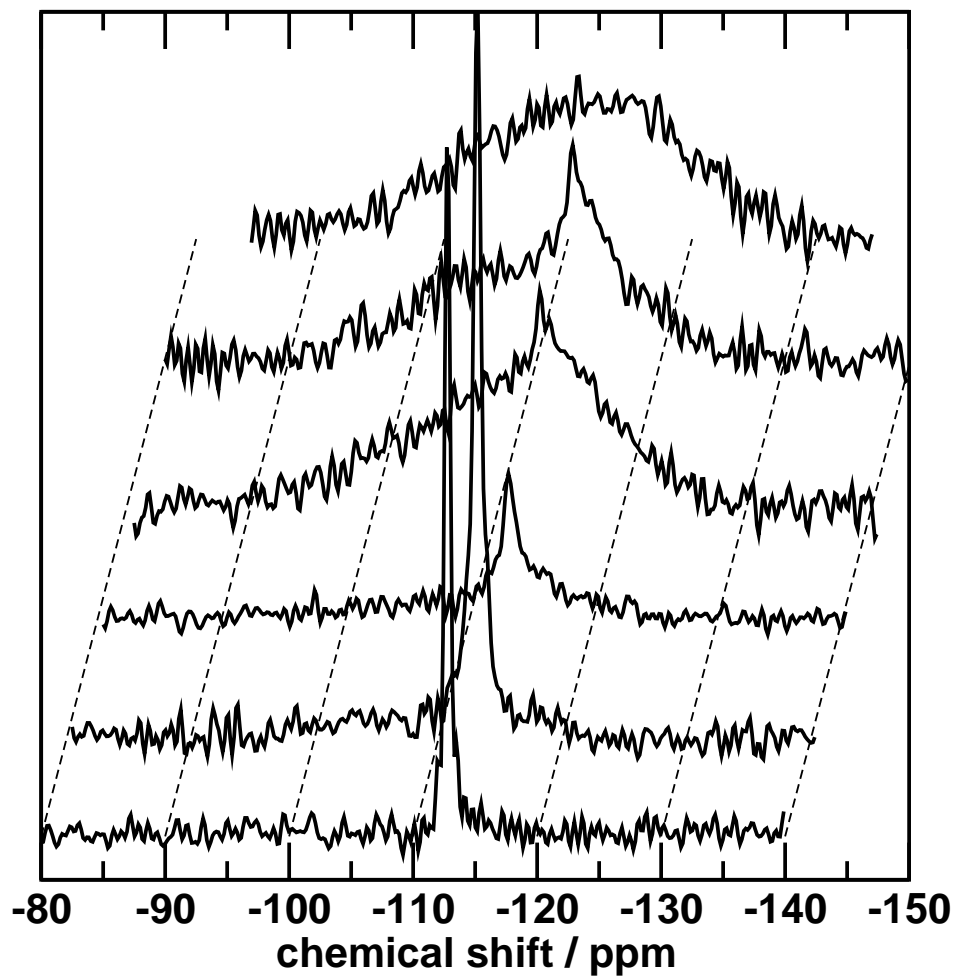
Fig. 2: ^{29}Si MAS NMR spectra of silica particles after (bottom to top) 0, 1, 8, 16, 32, 64 hours of ball milling. (The chemical shift scale corresponds to bottom spectrum only; all other spectra are shifted by 2.5 ppm each as indicated by the broken lines.).

Fig. 3: ^{29}Si MAS NMR spectra of ball-milled (32 hours) silica particles. The broken lines indicate the two components of a double-Gaussian fit (thin line). For comparison, spectra of amorphous silica (top, with single-Gaussian fit) and of coarse-grained silica (not ground, bottom) are shown.
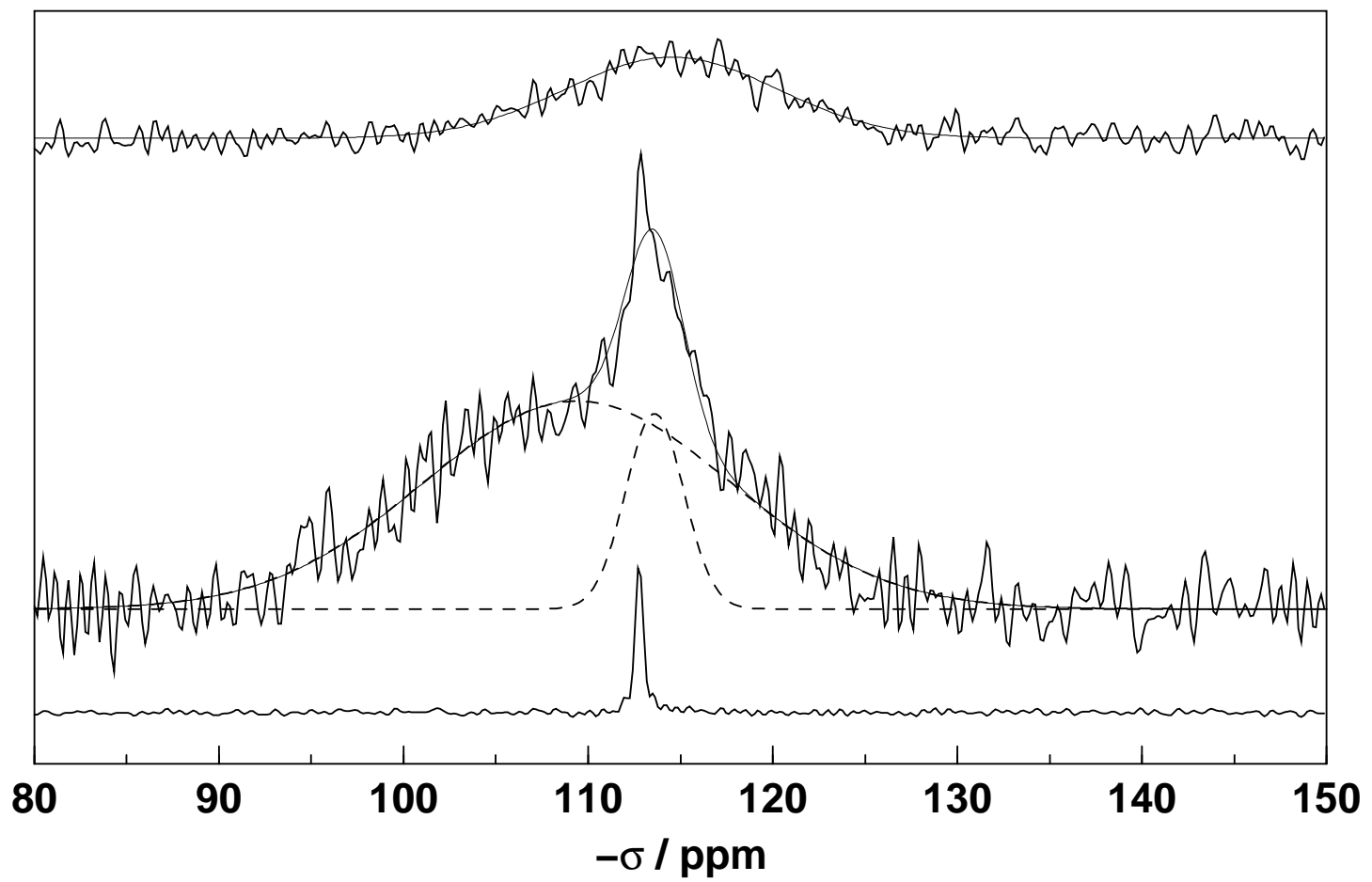
Fig. 4: Diffractograms of ball-milled (128 hours) silica after heat treatment at a rate of 15 K/min. Bottom to top: before annealing, at $\approx 240°$C, at $\approx 240°$C, and at $1\,025°$C. The grey curve displayed in the background is the diffractogram of coarse-grained quartz with its (100) and (101) reflections, for comparison.
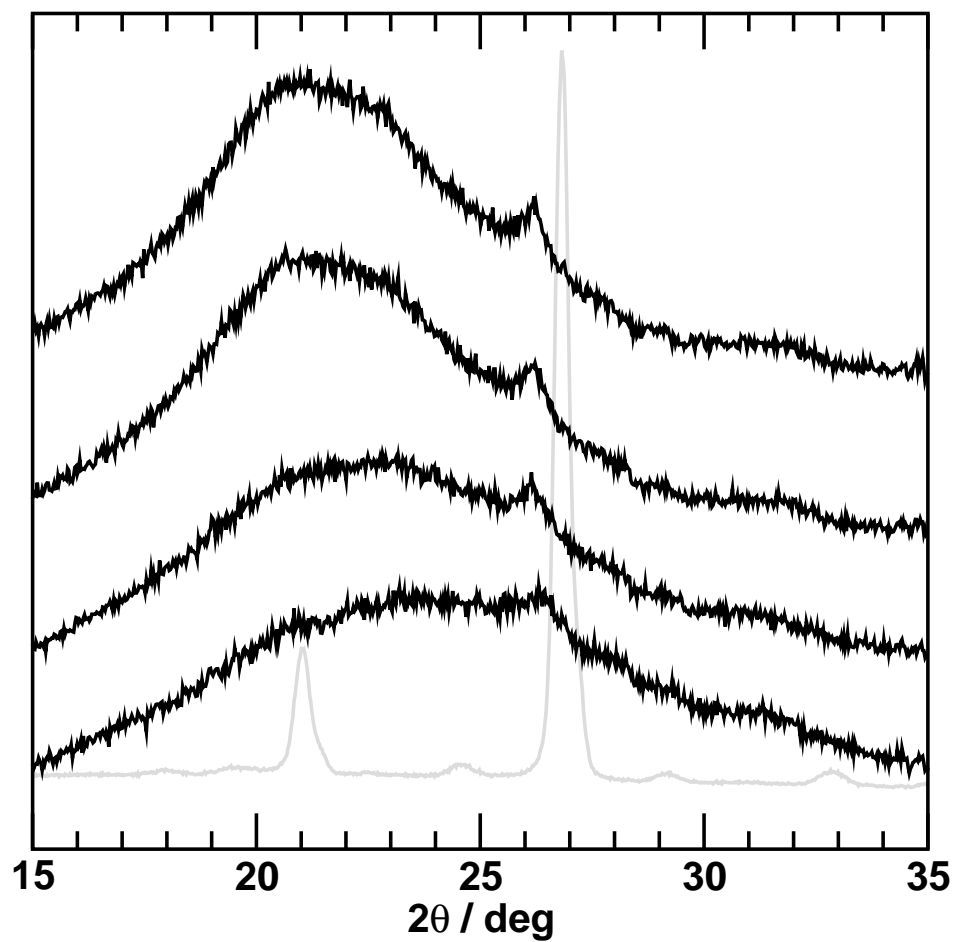
van Hoek, Winter; Fig. 1.

-80 -90 -100 -110 -120 -130 -140 -150
chemical shift / ppm

van Hoek, Winter; Fig. 2.

$-\sigma$ / ppm